Forward Time-of-Flight Detector Efficiency for CLAS12

D.S. Carman, Jefferson Laboratory

ftof_eff.tex

May 29, 2014

Abstract

This document details an absolute hit efficiency study of the FTOF panel-1a and panel-1b arrays in Sector 5 using data collected with a PCAL U/V coincidence trigger.

1 Introduction

This report details a measurement of the absolute hit efficiencies for the Forward Time-of-Flight (FTOF) counters for panel-1a and panel-1b. The average efficiencies for each counter are reported, as well as the efficiency vs. hit coordinate along the counter. These data were collected for Sector 5 using a PCAL low-threshold U/V coincidence trigger from cosmic ray runs taken in May 2014. For these runs the FTOF PMTs were reasonably well gain-matched, separately for panel-1a and panel-1b. The strategy to define the panel-1a (panel-1b) efficiency was to employ coincidences between panel-1b (panel-1a) and PCAL, and then to look for the hit in the FTOF array under study.

In this write-up, Section 2 provides an overview of the FTOF system and Section 3 details the relevant geometry of the FTOF arrays and the other Forward Carriage detectors. Section 4 provides a discussion of how the efficiency was defined and Section 5 details the measurement results. Finally, Section 6 contains a summary of the work and the conclusions.

Note that for these studies, the Low Threshold Cherenkov Counter (LTCC) boxes and the FTOF panel-2 arrays were not yet mounted to the Forward Carriage.

2 FTOF Overview

The CLAS12 detector is built around a six-coil toroidal magnet that divides the active detection area into six azimuthal regions called sectors. The torus coils are approximately planar. Each sector subtends an azimuthal range of 60° from the mid-plane of one coil to the mid-plane of the adjacent coil, where the sector mid-plane is an imaginary plane that bisects the azimuth of each sector.

The FTOF system is a major component of the CLAS12 forward detector used to measure the time-of-flight of charged particles emerging from interactions in the target. The average path length from the target to the FTOF counters is roughly 7 m. The requirements for the FTOF include excellent timing resolution for particle identification and good

segmentation to minimize counting rates and to provide for flexible triggering options. The system specifications call for an average time resolution of σ_{TOF}=80 ps at the more forward angles of CLAS12 ($\theta < 35°$) and 150 ps at larger angles ($\theta > 35°$).

In each of the six sectors of CLAS12, the FTOF system is comprised of three arrays of counters, named panel-1a, panel-1b, and panel-2. Each panel consists of a set of rectangular scintillators with a PMT on each end. Panel-1a and panel-1b refer to the counter arrays located at forward angles (roughly 5° to 35°) (where the two panels are necessary to meet the 80 ps average time resolution requirement) and panel-2 refers to the sets of counters at larger angles (roughly 35° to 45°). The positioning and attachment of the FTOF detector arrays to the Forward Carriage of CLAS12 are shown in Fig. 1. Each of the panel-1a arrays contains 23 counters, each of the panel-1b arrays contains 62 counters, and each of the panel-2 arrays contains 5 counters. A summary of the FTOF technical parameters is given in Table 1.

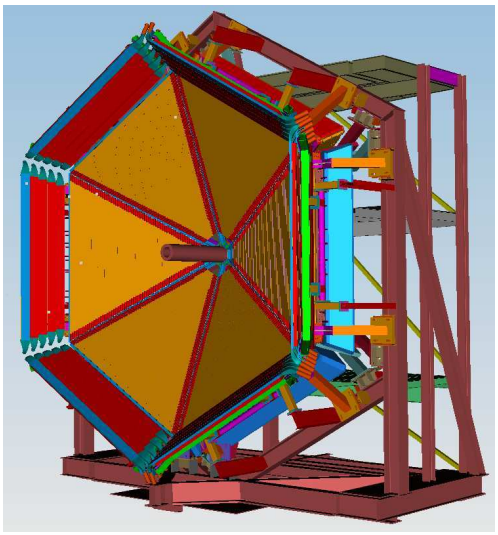

Figure 1: View of the FTOF counters for CLAS12 highlighting the location of the panel-1 and panel-2 counters. The panel-1b counter arrays are shown in orange and the panel-2 counter arrays, mounted around the perimeter of the Forward Carriage, are shown in red. The panel-1a counter arrays mounted just downstream of the panel-1b arrays are not visible in this picture. The Forward Carriage is roughly 10 m in diameter.

3 Nominal FTOF Geometry

Each of the six sectors on the Forward Carriage will ultimately contain five detector subsystems. Not including the FTOF panel-2 arrays mounted about the perimeter of the Forward Carriage (see Fig. 1), they include the LTCC, FTOF panel-1b, FTOF panel-1a, PCAL, and EC. The LTCC is the furthest upstream and the EC is the furthest downstream.

The geometry for each FTOF array is specified by a limited set of parameters. Figure 2 shows a view of the scintillator arrays in a single representative sector. This view is in the sector mid-plane and the key parameters used to specify the geometry are indicated. The nominal values of the FTOF geometry parameters for each sector are listed in Table 2. The

Parameter	Design Value
Panel-1a	
Angular Coverage	$\theta = 5^\circ \rightarrow 35^\circ$, ϕ : 50% at $5^\circ \rightarrow$ 85% at 35°
Counter Dimensions	$L = 32.3$ cm $\rightarrow 376.1$ cm, $w \times h = 15$ cm $\times$ 5 cm
Scintillator Material	BC-408
PMTs	EMI 9954A, Philips XP2262
Design Resolution	90 ps $\rightarrow$ 160 ps
Panel-1b	
Angular Coverage	$\theta = 5^\circ \rightarrow 35^\circ$, ϕ : 50% at $5^\circ \rightarrow$ 85% at 35°
Counter Dimensions	$L = 17.3$ cm $\rightarrow 407.9$ cm, $w \times h = 6$ cm $\times$ 6 cm
Scintillator Material	BC-404 (#1 $\rightarrow$ #31), BC-408 (#32 $\rightarrow$ #62)
PMTs	Hamamatsu R9779
Design Resolution	60 ps $\rightarrow$ 110 ps
Panel-2	
Angular Coverage	$\theta = 35^\circ \rightarrow 45^\circ$, ϕ : 85% at $35^\circ \rightarrow$ 95% at 45°
Counter Dimensions	$L = 371.3$ cm $\rightarrow 426.1$ cm, $w \times h = 22$ cm $\times$ 5 cm
Scintillator Material	BC-408
PMTs	Photonis XP4312B, EMI 4312KB
Design Resolution	145 ps $\rightarrow$ 160 ps

Table 1: Table of parameters for the scintillators, PMTs, and counters for the FTOF panel-1a, panel-1b, and panel-2 arrays.

definition of each of these parameters is included in Appendix A. Note that there are two values listed for gap_1b. The smaller value is the gap between counters mounted to a single backing structure and the larger value is the gap between counters on neighboring backing structures. Full details regarding the FTOF geometry are included in Ref. [1].

The left side of Fig. 3 shows a side view of the detector stack in one sector of the Forward Carriage, from the LTCC nearest the exit of the Region 3 drift chamber (left - shaded in pink) to the PCAL/EC furthest from the CLAS12 target (right - shaded in purple). The right side of Fig. 3 shows a side view of the active area of the Forward Carriage detectors from the FTOF panel-1b (left) to the EC (right). Note the solid angle mismatches of the different detectors. The middle of Fig. 3 shows a top view of the PCAL active area (in gray) with the FTOF panel-1a counters overlaid to again highlight the solid angle mismatches of the detectors on the Forward Carriage.

For this study, data were collected from the Forward Carriage detectors in Sector 5. In Fig. 1, Sector 5 is located at the "5 o'clock" position (i.e. the lower right sector).

4 FTOF Efficiency Definition

The basic definition of the FTOF detector efficiency for each counter is the number of reconstructed hits relative to the number of incident charged particles. However, determining

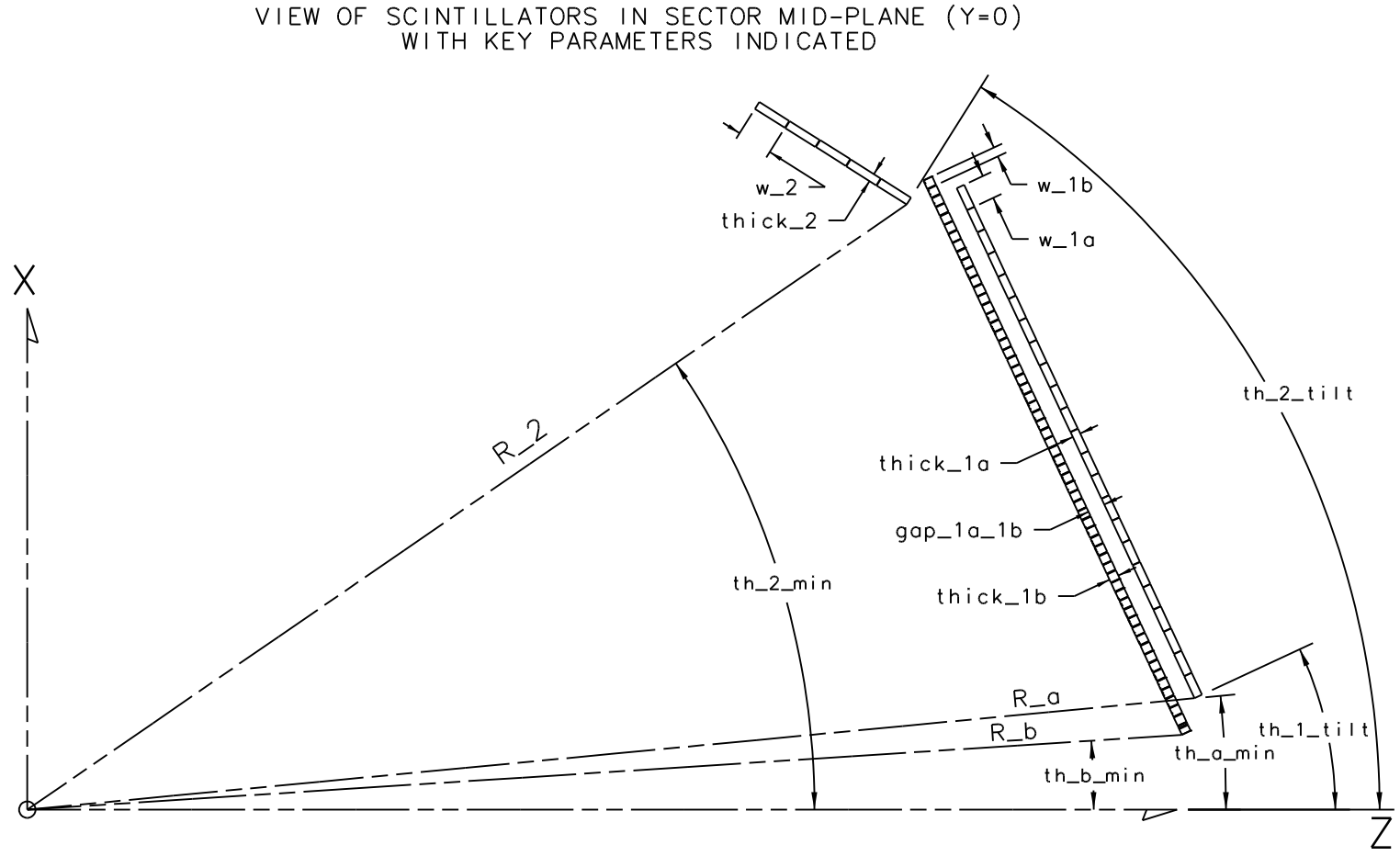

Figure 2: View of the FTOF scintillators for panel-1a, panel-1b, and panel-2 in the sector mid-plane with the key parameters indicated. The parameter definitions are included in Appendix A and the parameter values are given in Table 2.

Parameter	Nominal Value
R_a	726.689 cm
R_b	717.236 cm
th_a_min	5.453°
th_b_min	3.667°
th_1_tilt	25°
thick_1a	5.08 cm
w_1a	15.01 cm
thick_1b	6.0 cm
w_1b	6.0 cm
gap_1a_1b	10.717 cm
R_2	659.71 cm
th_2_min	34.698°
th_2_tilt	58.11°
thick_2	5.08 cm
w_2	22.0 cm
gap_1a	0.1384 cm
gap_1b	0.04 cm, 0.200 cm
gap_2	0.302 cm

Table 2: Table of the nominal geometry parameters for the CLAS12 FTOF detector system.

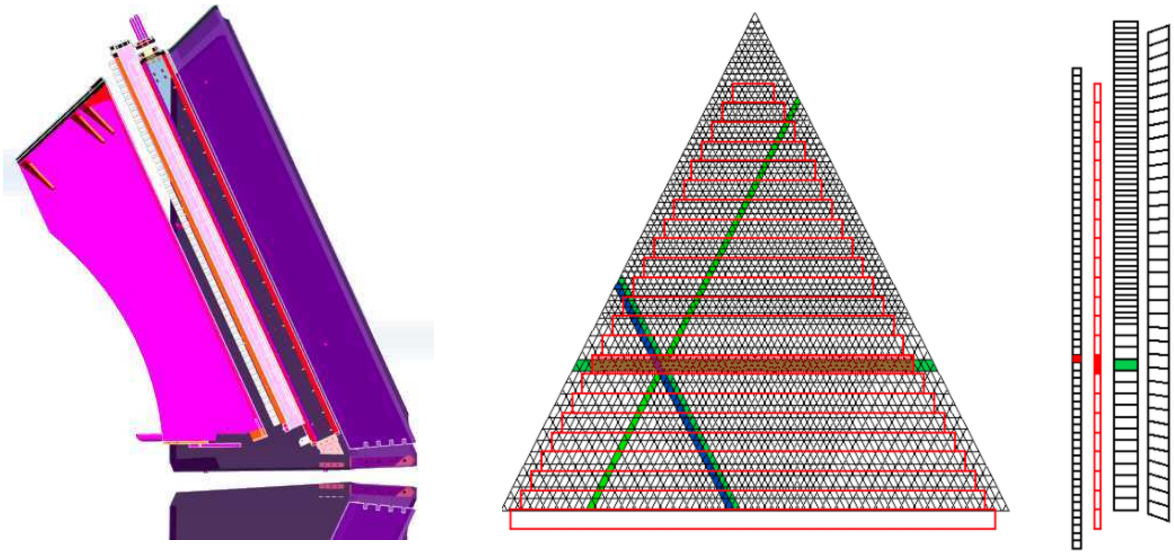

Figure 3: (Left) Side view of the detectors in one sector of the Forward Carriage with the LTCC on the left of the figure shaded in pink. (Right) Top view overlay of the active area of the PCAL (defined by its pixels in gray) and the FTOF panel-1a bars. On the right edge of the figure is a side view of the active areas of the panel-1b, panel-1a, PCAL, and EC going from left to right. The top of this side view matches the overlay picture in its orientation relative to the beamline.

an absolute detector efficiency requires some care. The most important factor to consider is the DAQ trigger definition employed for these cosmic ray studies that requires a PCAL U- and V-strip hit in coincidence above threshold. With this loose triggering condition, many muon tracks that hit the PCAL do not intercept the FTOF detectors. Ideally, to define the efficiencies for the scintillator bars we want to select a set of charged tracks normally incident upon the face of the FTOF that originated from the target region.

Because there are two layers of overlapping FTOF counters in front of the PCAL, we can improve our set of candidate tracks to study the FTOF panel-1a and panel-1b counter efficiency using the following definitions:

$$\varepsilon_i^{1a} = \frac{\text{FTOF}^{\text{1a}}\ \text{hit}_\text{i}}{\text{PCAL hit} \cdot \text{FTOF}^{\text{1b}}\ \text{hit}}, \quad i = 1 \rightarrow 23, \tag{1}$$

$$\varepsilon_i^{1b} = \frac{\text{FTOF}^{\text{1b}}\ \text{hit}_\text{i}}{\text{PCAL hit} \cdot \text{FTOF}^{\text{1a}}\ \text{hit}}, \quad i = 1 \rightarrow 62. \tag{2}$$

Thus to ensure the FTOF panel-1a array has the chance to register a hit, we require a hit in the FTOF panel-1b array that is just upstream. For studying the panel-1b counter efficiency, we can likewise require a hit in the panel-1a array that is just downstream. Note that these FTOF hit efficiencies are defined for each panel-1a counter ($i = 1 \rightarrow 23$ in Eq.(1)) and each panel-1b counter ($i = 1 \rightarrow 62$ in Eq.(2)).

In order to better define tracks that are normally incident on the face of the parallel FTOF arrays, we can improve our track selection by improving our definition of a "PCAL hit". Note that the PCAL does not have a projective geometry like the EC (see Fig. 3), whose UVW "pixels" project back to the CLAS12 center. Thus requiring a PCAL hit as a UVW pixel effectively defines a set of tracks normally incident on the FTOF arrays. We can further refine the PCAL hit definition requiring the following cuts:

1. $nhit = 1$ in each PCAL view (U, V, and W);
2. PCAL pixel matching condition;
3. PCAL energy for each hit strip $>$ threshold (i.e. just above pedestal).

Here the first requirement, $nhit = 1$, helps to define a good PCAL pixel by eliminating noise hits and to better define our incident track sample. The PCAL pixel matching condition requires that the single hit in the U-, V-, and W-layers overlap as a true hit pixel. Fig. 4 shows the geometrical pixel matching (or cluster) distribution and the cut employed [2]. The final requirement on the PCAL hit is to employ an ADC threshold cut just above pedestal in each U, V, and W layer, as shown in Fig. 5.

Turning attention to the FTOF hit definition in the denominator of Eqs.(1) and (2), there are several requirements necessary to ensure a clean event sample:

1. $nhit = 1$ in FTOF;
2. FTOF ADC cut;
3. FTOF edge coordinate cut;

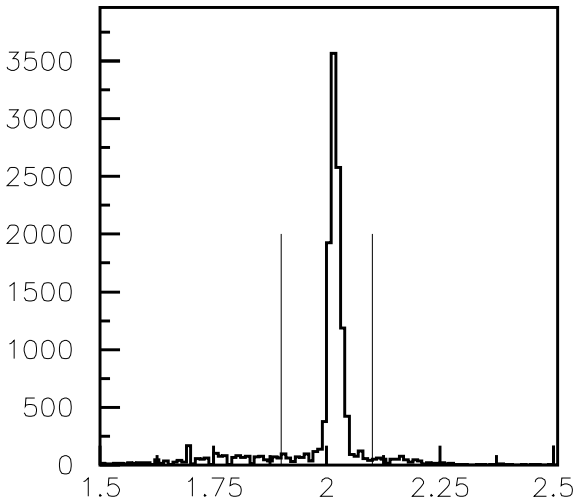

Figure 4: Pixel matching plot reconstructed for the PCAL hits for events with one hit in the U, V, and W layers. The peak at about 2 defines events that form a true PCAL pixel. The vertical lines show the cut employed to select PCAL pixel events.

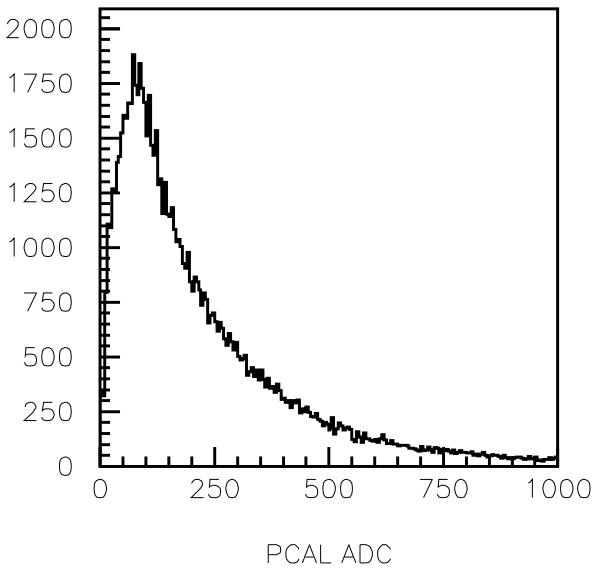

Figure 5: ADC distribution for a representative PCAL PMT ADC. The analysis employs a cut on the U, V and W PCAL ADC values to be greater than 30, which eliminates the ADC pedestal events.

4. FTOF/PCAL hit matching.

The first requirement is $nhit = 1$ in the FTOF array used in coincidence with the PCAL hit to define the incident charged particle sample. The goal is to remove any possible ambiguity in the track sample for measuring the panel-1a and panel-1b hit efficiencies by removing any hits from noisy PMTs or from FTOF hits that may not match to the PCAL hit that triggered the event. Fig. 6 shows the number of hits per event in the two FTOF arrays. As expected in panel-1b, the number of events with $nhit > 1$ is larger than for panel-1a due to the smaller counter widths (6 cm vs. 15 cm).

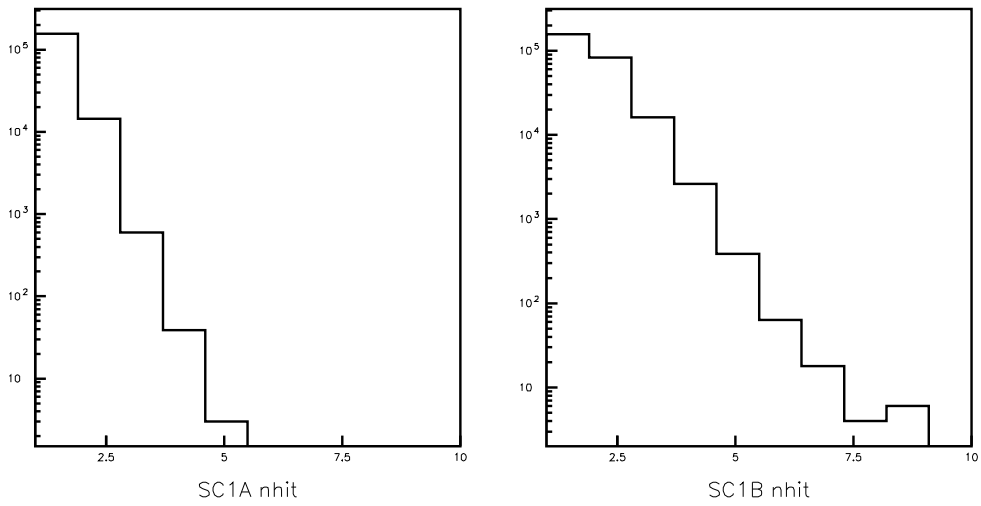

Figure 6: Number of hits (log y-scale) in panel-1a (left) and panel-1b (right) for each event.

The second requirement on the FTOF hit for the denominator of Eqs.(1) and (2) is an ADC cut. The data employed for this analysis was collected for Sector 5 after several iterations of the PMT gain matching algorithm. Fig. 7 shows the quality of the gain matching. Here the geometric ADC mean ($\sqrt{ADC_L \cdot ADC_R}$) of normally incident muons for panel-1a was adjusted to be in channel 800 and for panel-1b was adjusted to be in channel 2000. The log ratio plots (ADC_L/ADC_R) show good left/right gain balancing. To better define normally incident tracks on the face of the FTOF arrays and to eliminate tracks that only clip the corner of a counter and deposit less than "full" energy, the following geometric mean ADC cuts were employed:

$$\text{FTOF panel} - \text{1a} \qquad 600 < \langle ADC \rangle < 1300, \tag{3}$$

$$\text{FTOF panel} - \text{1b} \qquad 1600 < \langle ADC \rangle < 2700. \tag{4}$$

Note of course that as the panel-1b counters are square in cross section (6 cm $\times$ 6 cm), this cut only serves to eliminate the corner clippers at low pulse height and the showering events at larger pulse heights. Fig. 8 shows the geometric mean distributions for each FTOF counter in Sector 5 after HV gain matching with the applied cuts indicated.

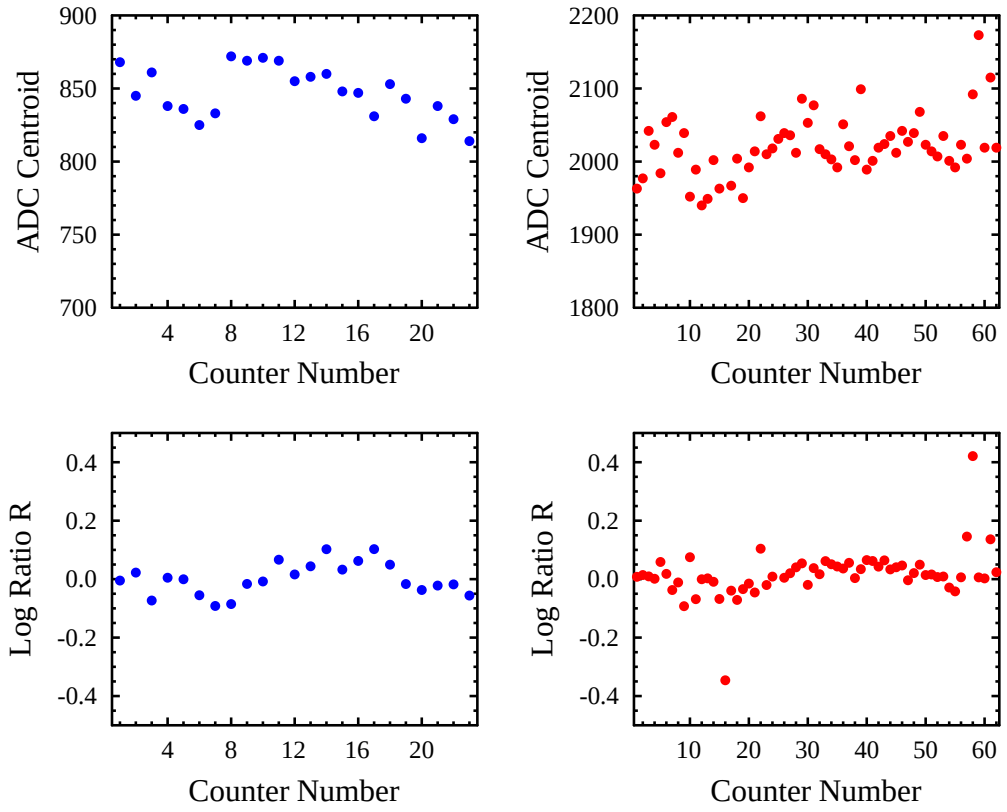

Figure 7: Summary of the quality of the gain matching of the panel-1a (left) and panel-1b (right) PMTs in Sector 5. The top plots show the fitted centroid of the geometric mean of the muon peak in the ADC spectrum and the bottom plots show the log ratio distributions that highlight the quality of the left and right PMT gain balancing for each counter.

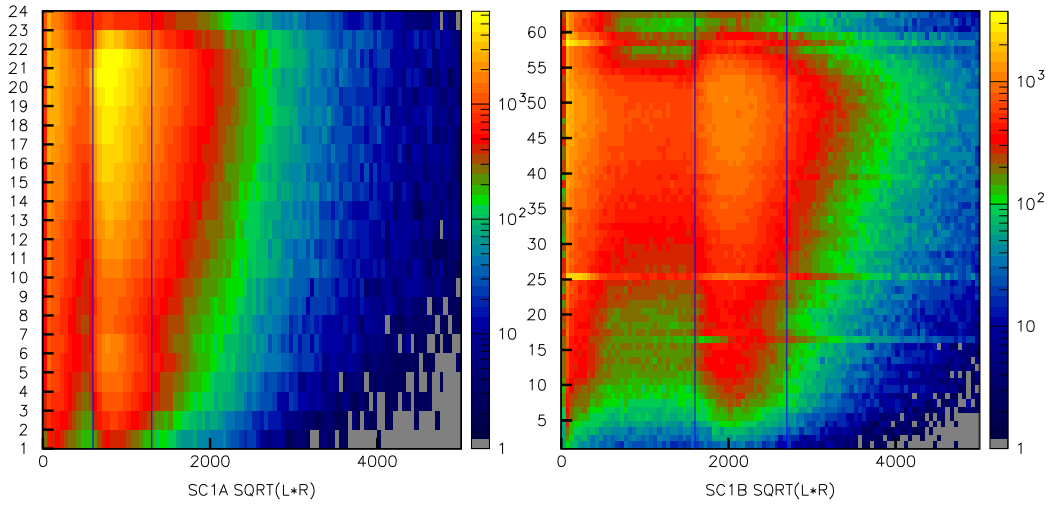

Figure 8: Distributions of the counter number vs. geometric mean for the Sector 5 panel-1a (left) and panel-1b (right) counters. The vertical lines show the ADC cuts employed.

The third requirement on the FTOF hit in the denominator of Eqs.(1) and (2) is designed to account for issues associated with the geometry mismatches between the FTOF panel-1a and panel-1b arrays. The FTOF hit coordinate along the scintillator bar, defined by:

$$x = \frac{1}{2v_{eff}}(TDC_L - TDC_R), \tag{5}$$

with v_{eff}=16 cm/ns, is required to be 5 cm away from the end of each counter as referenced to its nominal design length (see Ref. [1]). Note that the TDC difference distributions for each FTOF counter have been shifted to be centered about 0. Fig. 9 shows the counter number vs. the reconstructed hit coordinate along the counter for each FTOF array. Note that due to the geometrical mismatch between the PCAL and the FTOF arrays for the longest FTOF counters (see Fig. 3), the FTOF distributions are affected noticeably for the last few counters in panel-1a and panel-1b. Also note that the diagonal stripe across the reconstructed coordinate distributions is a direct result of the PCAL U/V trigger requirement bias.

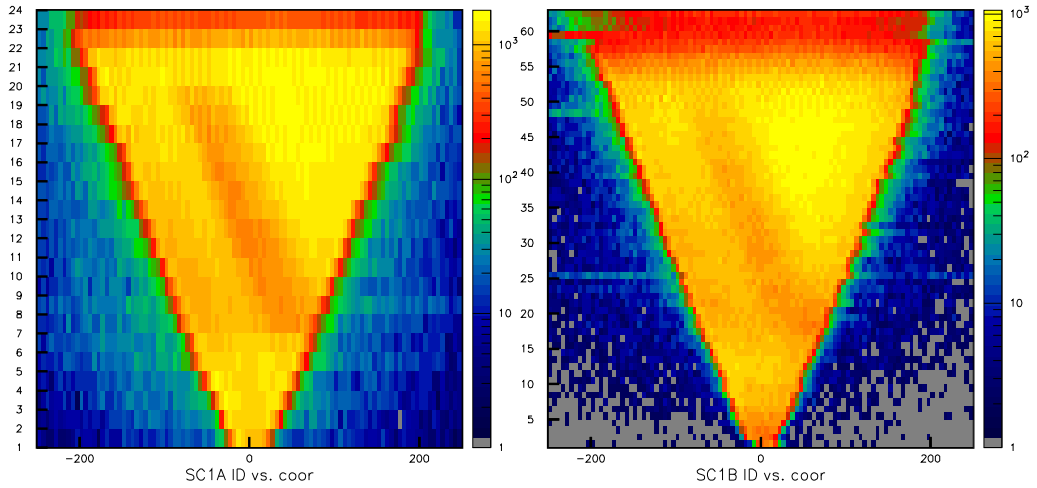

Figure 9: Distributions of counter number vs. coordinate along the bar (cm) for the Sector 5 panel-1a (left) and panel-1b (right) counters.

The final requirement on the FTOF hit definition in the denominator of Eqs.(1) and (2) is to ensure proper hit matching with the PCAL hit. Fig. 10 shows the correlation between the hit FTOF number and the hit PCAL U-strip (which runs parallel to the FTOF counters). This correlation shows that for a given PCAL U-strip hit, there is a tight requirement on the corresponding FTOF panel-1a and panel-1b counter hit for normally incident tracks. Note that the kinks in these distributions result from the pairing of the last 32 physical U-strips into 16 effective double-wide U strips in the PCAL module (see Ref. [3] for details).

Fitting these distributions gives the following expectations for the expected FTOF counter hit for a given PCAL U-strip hit for normally incident tracks,

$$\mathrm{FTOF}^{\mathrm{1a}}_{\mathrm{expected}} = 0.297 \cdot \mathrm{PCAL_U} - 2.647, \quad U\text{−strip} = 1 \rightarrow 52 \tag{6}$$

$$\mathrm{FTOF}^{\mathrm{1a}}_{\mathrm{expected}} = 0.593 \cdot \mathrm{PCAL_U} - 18.261, \quad U\text{−strip} = 53 \rightarrow 68 \tag{7}$$

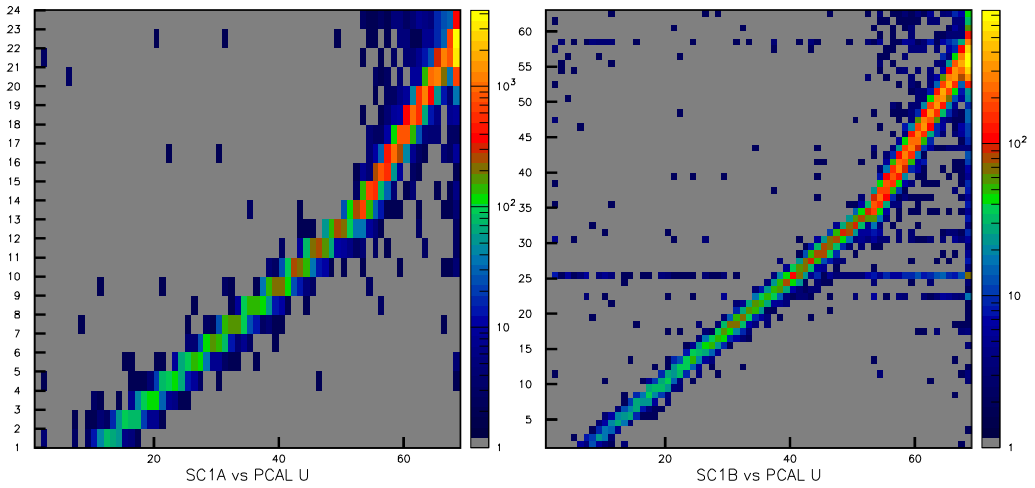

Figure 10: Distribution of FTOF counter number vs. PCAL U-strip number for panel-1a (left) and panel-1b (right).

$$\text{FTOF}^{\text{1b}}_{\text{expected}} = 0.748 \cdot \text{PCAL}_{\text{U}} - 4.852, \quad U-\text{strip} = 1 \rightarrow 52 \tag{8}$$

$$\text{FTOF}^{\text{1b}}_{\text{expected}} = 1.500 \cdot \text{PCAL}_{\text{U}} - 45.326, \quad U-\text{strip} = 53 \rightarrow 68. \tag{9}$$

The distributions of the difference between the expected FTOF counter hit and the actual counter hit are shown in Figs. 11 and 12. A $\pm 3\sigma$ cut is used to define the PCAL U-strip vs. FTOF counter matching for panel-1a and a $\pm 5\sigma$ cut is used for panel-1b due to the narrower extent of the counters and the increased distance away from the PCAL module (which allows for a greater range of incident muon track angles on the face of the FTOF - see Section 5).

Once the denominator of the efficiency definition (i.e. the sample of charged muons) is defined, we can then look to see if there is a hit in the FTOF array being considered. Here too we must be careful to define the hit characteristics so that we are properly measuring the hit efficiency. To that end, the following requirements are included:

- FTOF/PCAL matching;
- Multiple hit recovery.

The FTOF/PCAL matching amounts to the fact, based on the correlations of Fig. 10 for our defined event sample, for a given PCAL U-strip hit, we know where to look in the FTOF array for the presence of a hit based on Eqs.(6) to (9). For the panel-1a efficiency determination we apply at $\pm 3\sigma$ cut on the difference between the expected FTOF counter hit and the actual FTOF counter hit. However, for the panel-1b hit a complication arises that must be dealt with.

The approach to define the efficiency for the panel-1a counters was to use the PCAL U-strip hit to then determine if the associated panel-1a hit was present. This approach is sensible because the PCAL U-strips are narrower than the panel-1a counters even for the

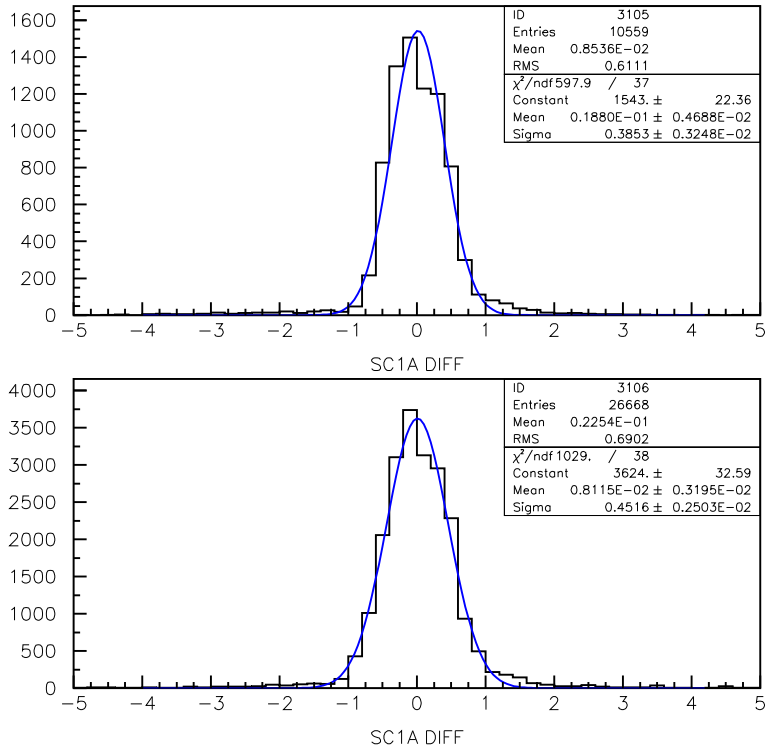

Figure 11: Distributions of the expected panel-1a hit counter (from Eqs.(6) and (7)) vs. the actual hit counter. The top plot is associated with PCAL U-strips $1 \rightarrow 52$ and the bottom plot is associated with PCAL U-strips $53 \rightarrow 68$.

last 16 coupled PCAL U-strips. In other words, there is a correspondence for each panel-1a counter with a PCAL U-strip. However, this same approach becomes problematic for the panel-1b efficiency determination for the longer U-strips. The coupled PCAL U-strips are effectively 9 cm wide, which is wider than the panel-1b counters (6 cm). Thus there is not a correspondence for each panel-1b counter with a PCAL U-strip. This gives rise to the noticeable discreteness of the difference distribution in Fig. 12, especially for the panel-1b hits associated with PCAL U-strips $53 \rightarrow 68$. A work-around is to consider instead the correlation between the sum of the PCAL U-strip and the FTOF panel-1a counter number with the FTOF panel-1b counter number.

Fig. 13 shows this correlation. If we define:

$$\mathrm{PCAL/FTOF_{hit}} = \mathrm{PCAL_U} + \mathrm{FTOF^{1a}_{hit}}, \tag{10}$$

then we have the following expectations for the FTOF panel-1b counter hit:

$$\mathrm{FTOF^{1b}_{expected}} = 0.565 \cdot (\mathrm{PCAL/FTOF_{hit}}) - 2.869, \quad \mathrm{PCAL/FTOF_{hit}} = 1 \rightarrow 65 \tag{11}$$

$$\mathrm{FTOF^{1b}_{expected}} = 0.900 \cdot (\mathrm{PCAL/FTOF_{hit}}) - 24.792, \quad \mathrm{PCAL/FTOF_{hit}} = 66 \rightarrow 91. \tag{12}$$

Fig. 14 shows the width of the distribution of the panel-1b predicted hit from the actual hit. Note that this distribution is, by design, more continuous compared to Fig. 12. If the

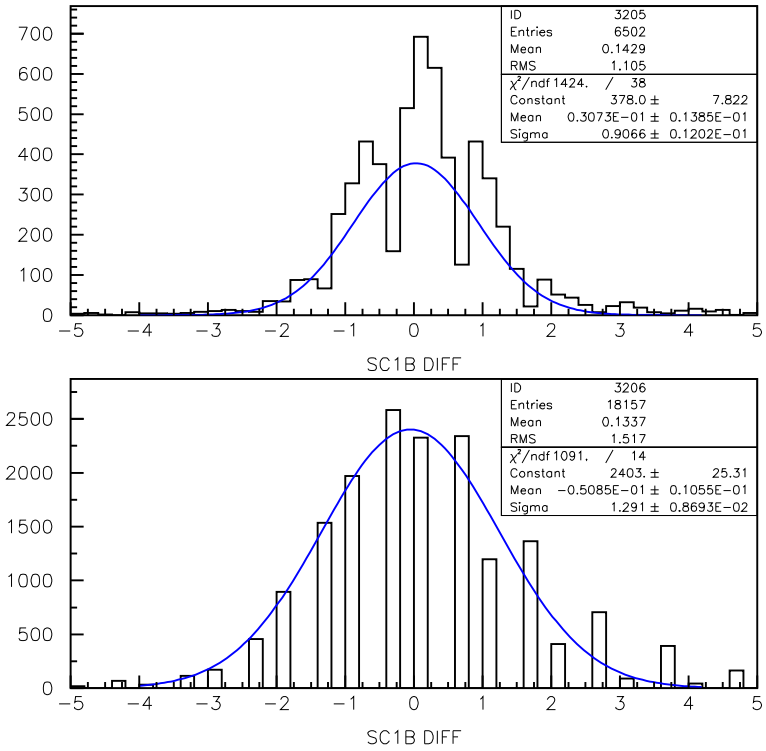

Figure 12: Distributions of the expected panel-1b hit counter (from Eqs.(8) and (9)) vs. the actual hit counter. The top plot is associated with PCAL U-strips $1 \rightarrow 52$ and the bottom plot is associated with PCAL U-strips $53 \rightarrow 68$.

actual panel-1b hit is found within $\pm 5\sigma$ of the expected hit, then the efficiency numerator of Eq.(2) is updated.

The second aspect of considering hits within the numerator of the efficiency definition is to deal with events in which $nhit > 1$. Table 3 provides a summary of Fig. 6. Again the fraction of panel-1b events with $nhit > 1$ compared to panel-1a is due to the narrower width of the panel-1b counters (6 cm vs. 15 cm).

$nhit$	panel-1a	panel-1b
1	91.2%	60.7%
2	8.4%	31.9%
3	0.3%	6.2%
≥ 4	0%	1.2%

Table 3: Number of hits per event for panel-1a and panel-1b.

The approach chosen for events with $nhit > 1$ is to see if the expected hit counter is present based on the $\pm 3\sigma$ requirement for panel-1a or the $\pm 5\sigma$ requirement for panel-1b among all of the hit counters of the event. With the numerator and denominator of our efficiency equations for panel-1a and panel-1b fully defined, we can study the measured efficiencies.

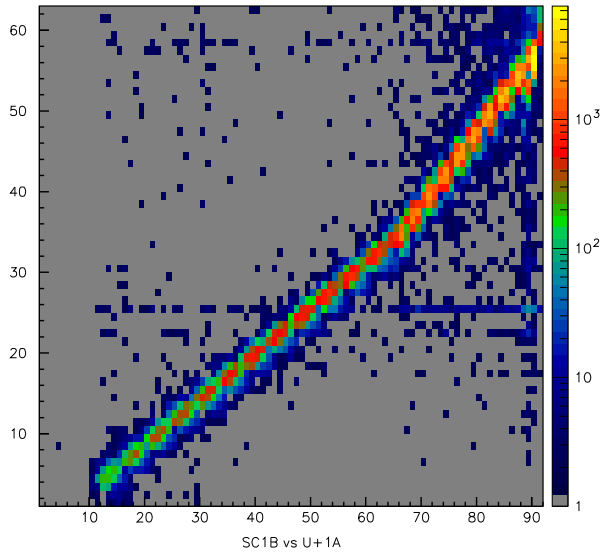

Figure 13: Distribution of the panel-1b counter number vs. the sum of the PCAL U-strip hit + panel-1a counter number.

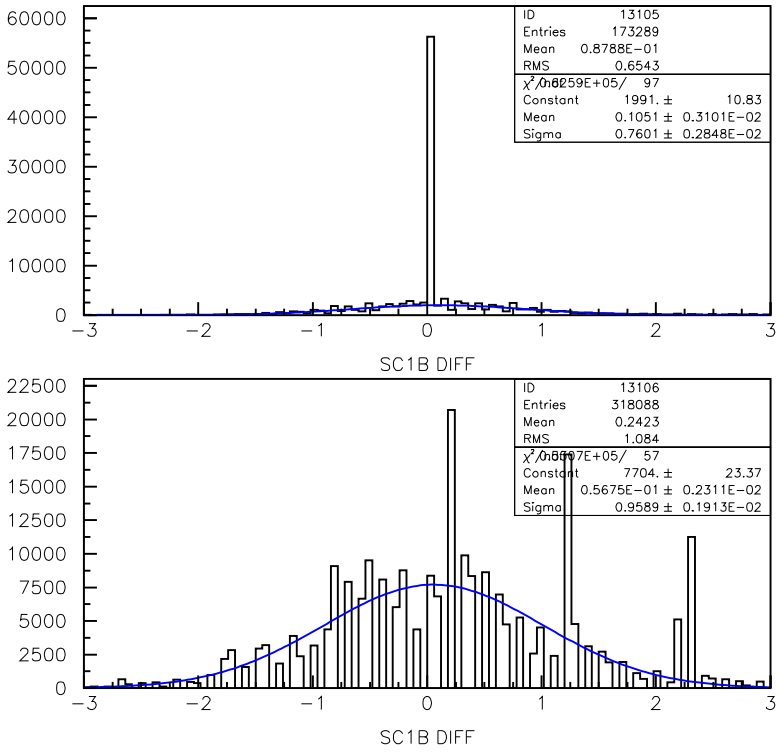

Figure 14: Distribution of the difference between the expected panel-1b counter hit from Eqs.(11) and (12) and the actual counter hit. The top plot is for PCAL U-strip + FTOF panel-1a hit 1 $\rightarrow$ 65. The bottom plot is for PCAL U-strip + FTOF panel-1a hit 66 $\rightarrow$ 91.

5 Results

With the requirements detailed in Section 4 on the numerator and denominator of the efficiency definitions of Eqs.(1) and (2), the efficiencies averaged over the full extent of each counter for panel-1a and panel-1b are shown in Figs. 15 and 16. These figures display the numerator, the denominator, and the ratio that defines the efficiency including a proper determination of the statistical uncertainties. For this analysis, nine separate runs of ∼1 to 1.5M events were added together. From these results, we note the following points:

1. For panel-1a, there is no trigger coverage for counters $22 \rightarrow 23$, so efficiencies cannot be determined.

2. For panel-1b, there is no trigger coverage for counters $57 \rightarrow 62$, so efficiencies cannot be determined.

3. For panel-1a there is no good PCAL pixel definition for counters $1 \rightarrow 3$, so the efficiency is not well defined.

4. For panel-1b, there is no good PCAL pixel definition for counters $1 \rightarrow 8$, so the efficiency is not well defined.

5. The average panel-1a hit efficiency from these data averaged over all counters is 99.5%.

6. The average panel-1b hit efficiency from these data averaged over all counters is 99.1%.

The FTOF hit efficiency can be studied vs. the hit coordinate along the scintillator. Using the hit coordinate definition from Eq.(5), Fig. 17 (left) shows the computed efficiency for panel-1a and Fig. 18 (left) shows the computed efficiency for panel-1b vs. the FTOF hit coordinate. Note that for the panel-1a efficiency, the plotted coordinate is from the hit panel-1b counter and for the panel-1b efficiency, the coordinate is from the hit panel-1a counter.

There is a second choice for computing the coordinate along the FTOF counters independent of the FTOF information, and that is from reconstructing the coordinate along the PCAL U-strip from the V and W-strip hit information. Using the details contained in Ref. [3], the U-strip hit coordinate is given by reconstructing the x-coordinates along the V-strip using:

$$v_j = (2j-1)\frac{\Delta}{\sin\alpha}, \qquad j = 1 \rightarrow 15 \tag{13}$$

$$= (j+14.5)\frac{\Delta}{\sin\alpha}, \quad j = 16 \rightarrow 62, \tag{14}$$

where j is the hit V-strip. Then we can compute:

$$x_v = \left[x_l - 77.0\frac{\Delta}{\sin\alpha}\right] + v_j. \tag{15}$$

Similarly the x-coordinate along the W-strip is given by:

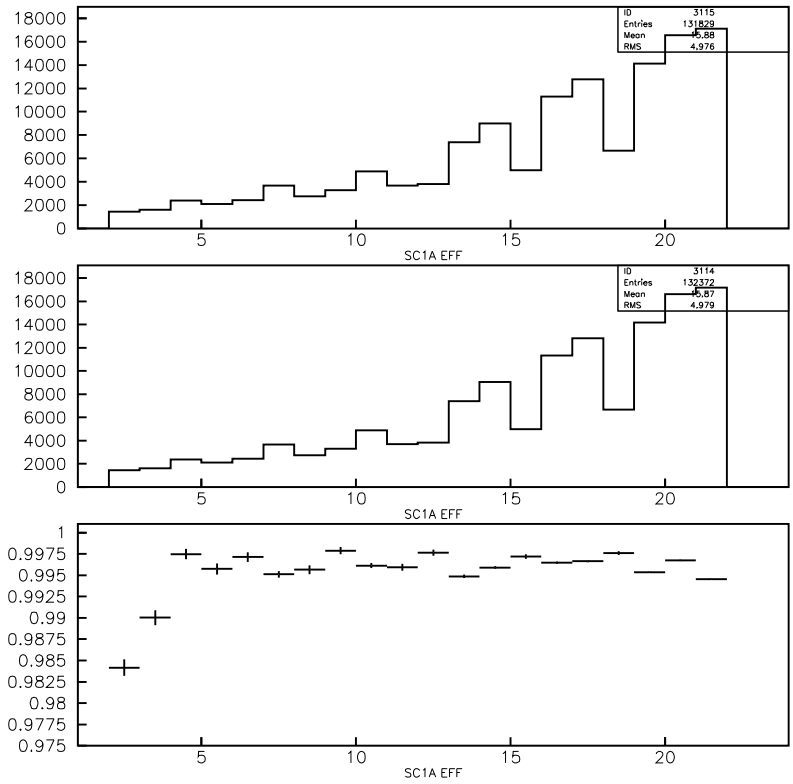

Figure 15: Panel-1a efficiency computed for each counter. The top distribution corresponds to the numerator and the middle distribution corresponds to the denominator of Eq.(1). The computed efficiency and statistical uncertainty is shown in the bottom plot.

$$w_j = (2j-1)\frac{\Delta}{\sin\alpha}, \qquad j = 1 \rightarrow 15 \tag{16}$$

$$= (j+14.5)\frac{\Delta}{\sin\alpha}, \quad j = 16 \rightarrow 62, \tag{17}$$

where j is the hit W-strip. Then we can compute:

$$x_w = \left[x_r + 77.0\frac{\Delta}{\sin\alpha}\right] + w_j. \tag{18}$$

Finally the coordinate along the U-strip is given by:

$$x_{PCALU} = -0.5\left[(x_v - 197.1) + (x_w + 197.1)\right]. \tag{19}$$

Here, $\Delta = 4.51$ cm is the PCAL strip width, $\alpha = 62.9°$ is the V and W strip angle relative to the U-strips, and $x_l = -x_r = 197.1$ cm is the half width of the PCAL module base length. The panel-1a efficiency vs. U-strip hit coordinate is shown in Fig. 17 (right) and the panel-1b efficiency vs. U-strip hit coordinate is shown in Fig. 18 (right).

From these results, there are several things to note:

1. The FTOF efficiency across the face of the arrays is essentially 100% to within statistical uncertainties. The efficiency drops near the very edges of panel-1a due to the fact

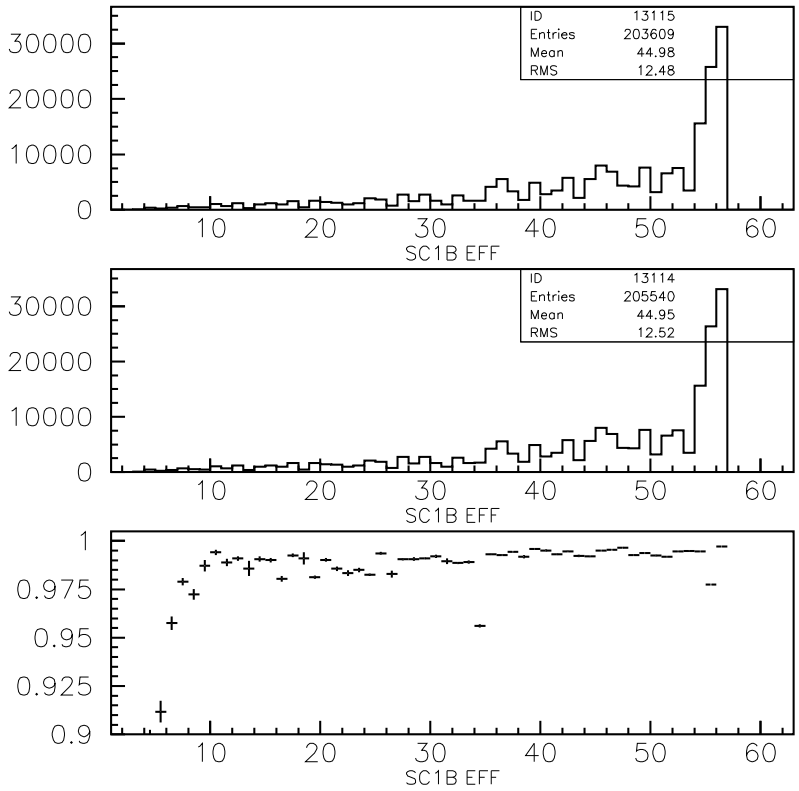

Figure 16: Panel-1b efficiency computed for each counter. The top distribution corresponds to the numerator and the middle distribution corresponds to the denominator of Eq.(2). The computed efficiency and statistical uncertainty is shown in the bottom plot.

that the panel-1b scintillators are longer than the panel-1a scintillators. The efficiency along one edge of panel-1b drops off due to the geometrical mismatch of the PCAL and FTOF arrays, with the PCAL centerline shifted by ∼1 cm relative to the FTOF centerline (see Ref. [1] for details).

2. The algorithm to compute the efficiency is based on looking for the presence of a panel-1a hit or a panel-1b hit based on an expectation from a PCAL U-strip hit (for panel-1a) or the summed PCAL U-strip hit + FTOF panel-1a hit (for panel-1b). If a neighboring hit counter relative to the expected counter is noisy or has a muon hit of its own, the inefficiency in the expected counter could be missed given the $\pm 3\sigma$ matching requirement for panel-1a or the $\pm 5\sigma$ matching requirement for panel-1b.

3. The FTOF panels are not active across 100% of their radial extents due to the gaps between neighboring counters, as well as the wrapping materials. To set a scale for the expected inefficiency due to this geometrical effect, the relevant numbers can be extracted from Ref. [1].

$$\text{panel} - \text{1a inefficiency} = \frac{\text{gaps} + \text{wrapping materials}}{\text{counter radial extent}} = \frac{4.237 \text{ cm}}{349.237 \text{ cm}} = 1.2\% \quad (20)$$

$$\text{panel} - \text{1b inefficiency} = \frac{7.228 \text{ cm}}{379.228 \text{ cm}} = 1.9\% \quad (21)$$

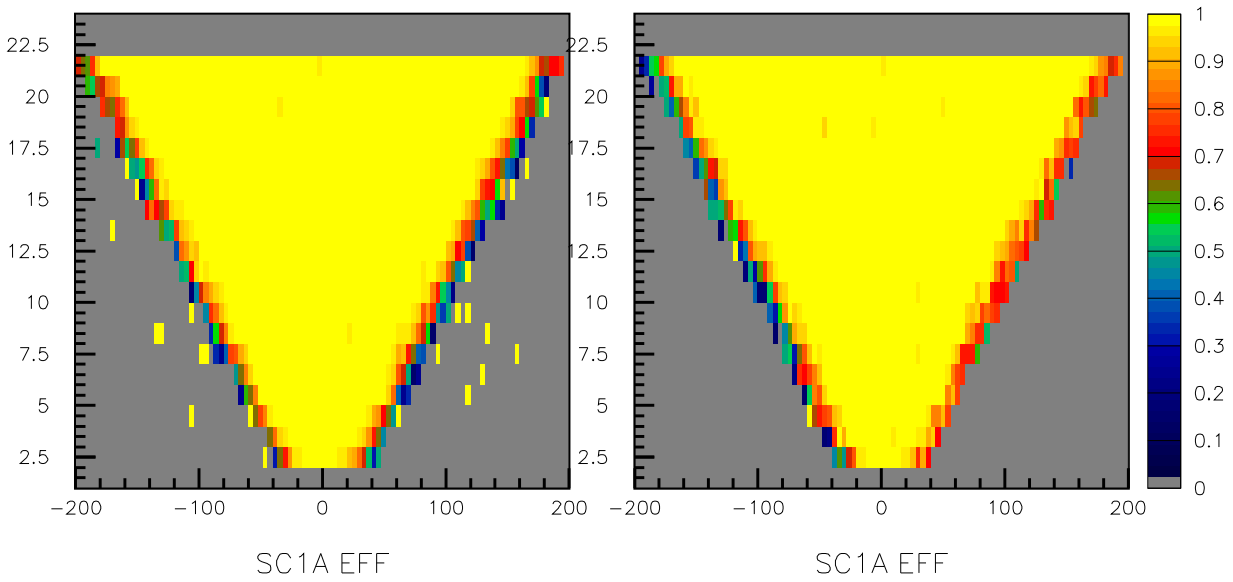

Figure 17: Panel-1a absolute efficiency in terms of counter number vs. panel-1b hit coordinate (left) and vs. PCAL U-strip hit coordinate (right). (Coordinates in cm)

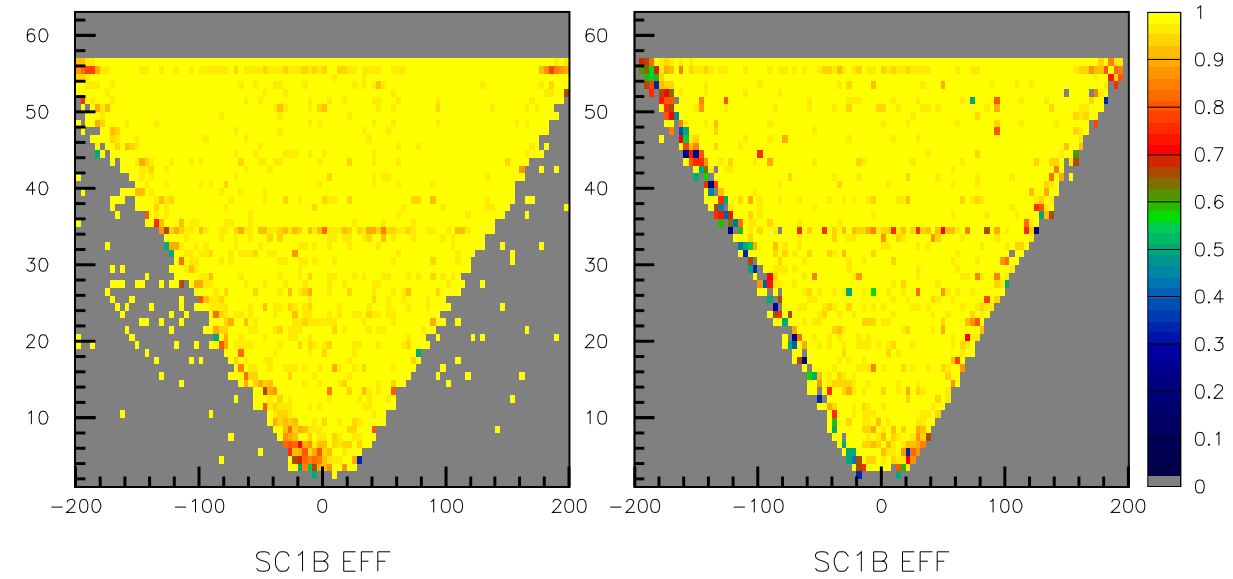

Figure 18: Panel-1b absolute efficiency in terms of counter number vs. panel-1a hit coordinate (left) and vs. PCAL U-strip hit coordinate (right). (Coordinates in cm)

Of course, the level of inefficiency seen from the measurements can be expected to be somewhat different due to the FTOF hit requirement in the denominator of Eqs.(1) and (2), and due to the fact that tracks can have a range of incidence angles with respect to the normal to the FTOF counter plane. However, we should expect a bigger inefficiency for panel-1b relative to panel-1a due to this geometrical effect and that is seen in the average efficiencies.

A crude determination of the track incident angles relative to the normal to the FTOF arrays can be determined using the hit information in the FTOF and the PCAL. For the panel-1a efficiency studies, using the coordinate information from panel-1b and PCAL, the range of incident angles on panel-1a is determined by:

$$\theta_{1a} = \text{atan}\left(\frac{y_{1b} - y_{PCALU}}{d_{1b-PCAL}}\right), \tag{22}$$

where y_{1b} and y_{PCALU} are the hit coordinates from FTOF panel-1b and the PCAL U-strip (see Appendix B), respectively, along the sector midplane line. $d_{1b-PCAL}$=35.41 cm is the distance from the face of FTOF panel-1b to the face of the PCAL active layer. For the panel-1b efficiency studies, using the coordinate information from panel-1a and PCAL, the range of incident angles on panel-1b is determined by:

$$\theta_{1b} = \text{atan}\left(\frac{y_{1a} - y_{PCALU}}{d_{1a-PCAL}}\right), \tag{23}$$

where y_{1a} and y_{PCALU} are the hit coordinates from FTOF panel-1a and the PCAL U-strip (see Appendix B), respectively, along the sector midplane line. $d_{1a-PCAL}$=18.69 cm is the distance from the face of FTOF panel-1a to the face of the PCAL active layer. Fig. 19 shows that the range of muon incident angles upon the face of the FTOF arrays using the cuts and requirements defined is in the range from $\pm 10^\circ \rightarrow \pm 15^\circ$.

4. Looking at the panel-1b efficiency plot of Fig. 18, there are slight inefficiencies seen for counters #34 ($\langle\varepsilon\rangle$ = 95.5%) and #55 ($\langle\varepsilon\rangle$ = 97.5%). The inefficiency associated with panel-1b counter #34 is likely not real as this counter spans the region where the PCAL transitions from single U-strip readout to double U-strip readout, so there is likely some small geometrical mismatch in our algorithm cuts. For counter #55, the efficiency may be affected by the fact that the PMT for panel-1b #58R in Sector 5 is hot or the fact that it is just on the edge of the acceptance of the trigger defined by the PCAL, although these are just speculations.

6 Summary and Conclusions

Using data accumulated for Sector 5 on the Forward Carriage over multiple runs, defined by a low threshold PCAL U/V trigger with gain matched arrays for the FTOF panel-1a and panel-1b counters, the average efficiencies of the FTOF counters and the efficiencies vs. coordinate along the counters have been measured. The absolute efficiencies have been

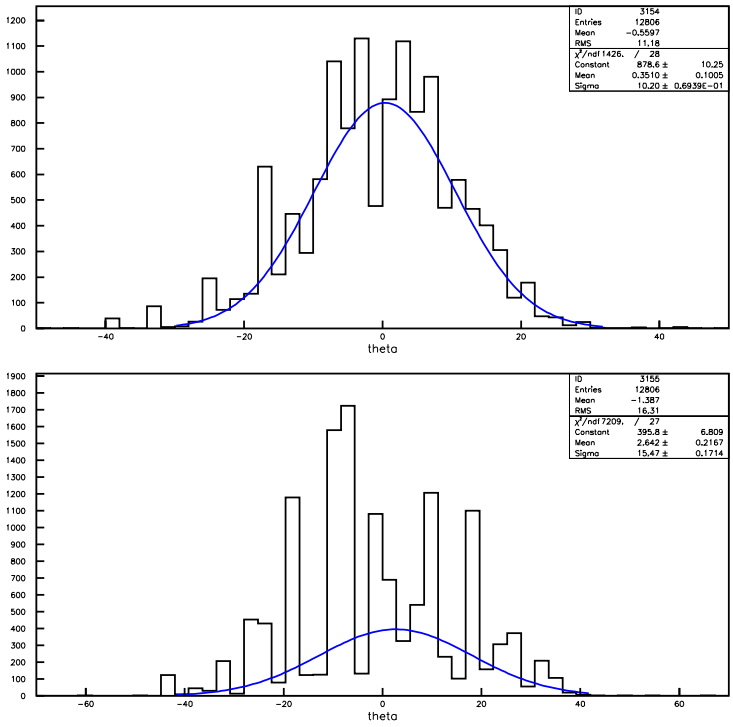

Figure 19: Distribution of track angles (in degrees) incident upon panel-1a computed using Eq.(22) (top) and upon panel-1b computed using Eq.(23).

shown to be greater than 99% over the face of the FTOF counters. Inefficiencies at the level of 20% to 50% are seen at the ends of the bars spanning ≈10 cm from the PMTs. This effect was seen at both ends of the panel-1a bars but on only one end of the panel-1b bars. Given that the effect is the same for all counters independent of length, the apparent inefficiency is certainly not due to attenuation length effects. It is more likely due to bias in the PCAL U/V trigger and due to the geometrical mismatch between the Forward Carriage detector arrays for FTOF panel-1b, FTOF panel-1a, and PCAL. The algorithms developed here can also be applied to study the FTOF hit efficiencies for the other sectors on the Forward Carriage to explore their performance.

Appendix A

The definitions of the FTOF system geometry parameters labeled in Figure 2 are as follows:

- **R_a** - distance from the nominal CLAS12 center to the small angle upstream edge of panel-1a counter #1.
- **R_b** - distance from the nominal CLAS12 center to the small angle upstream edge of panel-1b counter #1.
- **th_a_min** - polar angle of the ray marking R_a.
- **th_b_min** - polar angle of the ray marking R_b.
- **th_1_tilt** - tilt angle of the panel-1a and panel-1b arrays relative to a line perpendicular to the z-axis (or electron beamline).
- **thick_1a** - thickness of the panel-1a scintillators.
- **w_1a** - width of the panel-1a scintillators.
- **thick_1b** - thickness of the panel-1b scintillators.
- **w_1b** - width of the panel-1b scintillators.
- **gap_1a_1b** - separation between panel-1a and panel-1b.
- **R_2** - distance from the nominal CLAS12 center to the small angle upstream edge of panel-2 counter #1.
- **th_2_min** - polar angle of the ray marking R_2.
- **th_2_tilt** - tilt angle of the panel-2 arrays relative to a line perpendicular to the z-axis.
- **thick_2** - thickness of the panel-2 scintillators.
- **w_2** - width of the panel-2 scintillators.
- **gap_1a** - gap between neighboring panel-1a counters (not shown).
- **gap_1b** - gap between neighboring panel-1b counters (not shown).
- **gap_2** - gap between neighboring panel-2 counters (not shown).

Appendix B

The hit coordinate along the midplane of panel-1a is given by:

$$y1a = (\mathrm{FTOF}^{\mathrm{1a}}_{\mathrm{hit}} - 1)(\mathrm{wid\_1a} + \mathrm{gap\_1a}) + 0.5 \cdot \mathrm{wid\_1a} + y_{off1a}, \tag{24}$$

where y_{off1a} is the offset of the edge of panel-1a relative to the beamline and FTOF^{1a}_{hit} is the hit panel-1a counter number. The values of the other parameters are given in Table 2.

The hit coordinate along the midplane of panel-1b is given by:

$$\begin{aligned} y1b = (2 \cdot \mathrm{wid\_1b} + \mathrm{gap\_1b(1)} + \mathrm{gap\_1b(2)}) \cdot (N_{pair} - 1) + \\ (\mathrm{wid\_1b} + \mathrm{gap\_1b(1)}) \cdot N_{member} + y_{off1b}, \end{aligned} \tag{25}$$

where

$$N_{pair} = \frac{\left(mod(\mathrm{FTOF}^{\mathrm{1b}}_{\mathrm{hit}}, 2) + \mathrm{FTOF}^{\mathrm{1b}}_{\mathrm{hit}}\right)}{2} \tag{26}$$

$$N_{member} = mod(\mathrm{FTOF}^{\mathrm{1b}}_{\mathrm{hit}} + 1, 2). \tag{27}$$

Here y_{off1b} is the offset of the edge of panel-1a relative to the beamline and FTOF^{1b}_{hit} is the hit panel-1b counter number. The values of the other parameters are given in Table 2.

The hit coordinate along the midplane of the PCAL is given by:

$$y_v = yh - (x_{PCALU} - x_v)\tan\alpha \tag{28}$$

$$y_w = yh - (x_w - x_{PCALU})\tan\alpha \tag{29}$$

$$y_{PCALU} = (PCAL_U - 1)\Delta + 0.5\Delta, \quad U\mathrm{-strip} = 1 \rightarrow 52 \tag{30}$$

$$y_{PCALU} = 52\Delta + [2 \cdot (PCAL_U - 52) - 1]\,\Delta \quad U\mathrm{-strip} = 53 \rightarrow 68, \tag{31}$$

where $\Delta = 4.51$ cm is the PCAL strip width, $\alpha = 62.9°$ is the V and W strip angle relative to the U-strips, and yh=94.4 cm is the height of the corner of PCAL base relative to the x-axis in the PCAL local coordinate system (see Ref. [3]). Note that the coordinates x_v, x_w, and x_{PCALU} are defined in Section 5.

References

[1] D.S. Carman, *Forward Time-of-Flight Geometry for CLAS12*, CLAS12-Note 2014-005, (2014).

[2] L.C. Smith, FORTRAN function *good_uvw_pc*, private communication, (2014).

[3] G. Asryan *et al.*, *The Geometry of the CLAS12 Preshower Calorimeter*, (2014).